

Magnetic properties and nonmagnetic phases formation in $(\text{Fe}/\text{Si})_n$ films

Cite as: J. Appl. Phys. **104**, 094703 (2008); <https://doi.org/10.1063/1.3005973>

Submitted: 03 January 2008 • Accepted: 09 September 2008 • Published Online: 06 November 2008

S. N. Varnakov, S. V. Komogortsev, S. G. Ovchinnikov, et al.



View Online



Export Citation

ARTICLES YOU MAY BE INTERESTED IN

[Iron silicide formation at different layers of \$\(\text{Fe}/\text{Si}\)_3\$ multilayered structures determined by conversion electron Mössbauer spectroscopy](#)

Journal of Applied Physics **116**, 023907 (2014); <https://doi.org/10.1063/1.4887522>

[Formation and ferromagnetic properties of FeSi thin films](#)

Journal of Applied Physics **113**, 17C306 (2013); <https://doi.org/10.1063/1.4800839>

[Interface and bulk magnetization dynamics in biaxial Fe/Cr structures induced by ultrashort optical pulses](#)

Journal of Applied Physics **104**, 083918 (2008); <https://doi.org/10.1063/1.3005884>

Lock-in Amplifiers
up to 600 MHz



Zurich
Instruments



Magnetic properties and nonmagnetic phases formation in $(\text{Fe}/\text{Si})_n$ filmsS. N. Varnakov,^{1,2,a)} S. V. Komogortsev,¹ S. G. Ovchinnikov,¹ J. Bartolomé,^{3,b)} and J. Sesé⁴¹*Kirensky Institute of Physics, Siberian Division, Russian Academy of Sciences, Akademgorodok, Krasnoyarsk 660036, Russia*²*Siberian Aerospace University, pr. im. gazety "Krasnoyarskii rabochii" 31, Krasnoyarsk 660014, Russia*³*Instituto de Ciencia de Materiales de Aragón, Departamento de Física de la Materia Condensada, CSIC-Universidad de Zaragoza, Zaragoza 50009, Spain*⁴*Instituto de Nanociencia de Aragón, Departamento de Física de la Materia Condensada, Universidad de Zaragoza, Zaragoza 50009, Spain*

(Received 3 January 2008; accepted 9 September 2008; published online 6 November 2008)

The magnetization of Fe/Si multilayers, grown by thermal evaporation in an ultrahigh vacuum system, was investigated at high temperatures. Magnetization and its temperature dependence up to a high temperature of 800 K depend on individual Fe layer thickness d_{Fe} . This dependence is the result of the formation of an Fe–Si interface layer (nonmagnetic phase) during the synthetic procedure. The fraction of this Fe–Si nonmagnetic phase is estimated versus d_{Fe} . At temperatures higher than 400 K an irreversible decrease in the magnetization occurs. A quantitative analysis of this irreversible behavior is proposed in terms of an exponential diffusion-like kinetic equation for the reaction that produces the Fe–Si nonmagnetic phase. The coefficients of the rate equation are the activation energy E_a and the prefactor D_0 , which have been determined for different d_{Fe} . © 2008 American Institute of Physics. [DOI: 10.1063/1.3005973]

I. INTRODUCTION

Interest in $(\text{Fe}/\text{Si})_n$ multilayer magnetic structures has increased in recent years as a result of their unique physical properties and prospects for practical applications.^{1–9} The transport of spin-polarized electrons across a ferromagnetic/semiconductor interface with a Si semiconductor layer is also interesting for spintronics because it opens the possibility of integrating the spin degree of freedom into Si-based technology.

In addition to dimensional quantum effects and the inter-layer magnetic coupling effect, the physical properties of the multilayer structure $(\text{Fe}/\text{Si})_n$ are governed by the iron silicide phases formed at the interface.¹⁰ Thus, $(\text{Fe}/\text{Si})_n$ films with controlled nanometer-thickness layers are good systems in studying iron silicide synthesis by solid-state reactions.

According to the Fe–Si phase diagram¹¹ there are two stable silicide phases (FeSi and FeSi₂) below 800 °C. The solubility of Si in Fe is about 26 at. % in this temperature range. As the composition of Fe_{1–x}Si_x with x close to 0.25 is approached [i.e., the α -Fe (bcc structure) region on the phase diagram], the film transforms into an ordered structure with a cubic unit cell of the Bi₃F type. The considerable contribution of the interface to the total energy of $(\text{Fe}/\text{Si})_n$ films with nanometric layers results in the formation of phases that do not exist on the equilibrium bulk phase diagram. The identification and study of such silicide phases with diffraction techniques are difficult because of their small volume.

From experimental investigations of the structure and composition of Fe/Si films (by Mössbauer spectroscopy) it was concluded that the following stable phases are formed at

the Fe/Si interface: magnetic solid solutions Fe–Si,^{12–16} nonmagnetic silicides ϵ -FeSi, β -Fe₂Si,^{12,15,16} and metastable silicides Fe₃Si,^{12,13} α -FeSi₂,^{12,15} and c -FeSi.^{12,14,15} In Ref. 14 it was shown that for Si layers up to 1.5 nm in Fe/Si multilayers grown by molecular-beam epitaxy (MBE), the whole intermediate layer between Fe layers is formed by crystal monosilicide c -FeSi (metastable metal phase with a structure of the CsCl type), with the lattice epitaxially arranged with the neighboring Fe layers. This conclusion is restricted to the growth method and sample quality described in Ref. 14, and cannot be generalized to all Fe/Si structures.

Nonmagnetic silicide phases in $(\text{Fe}/\text{Si})_n$ films are formed both during and after the synthetic procedure. The volume of nonmagnetic phases is determined both by the equilibrium phase diagram and the kinetics of phase formation, because the time required to reach thermodynamic equilibrium at room temperature (RT) is very long. The high concentration of structural defects in $(\text{Fe}/\text{Si})_n$ films causes considerable changes in the kinetic factors of the various atomic transport processes existent in the films, in comparison with diffusion in bulk samples.¹⁷

The objective of this work is to find the relative amount of nonmagnetic phases, which are formed both during the synthetic procedure of $(\text{Fe}/\text{Si})_n$ films and, as a result, of high temperature silicide formation processes, using magnetic measurements. We study *in situ* temperature and time dependences of film magnetization during annealing in a superconducting quantum interference device (SQUID) magnetometer.

II. EXPERIMENTAL

The starting samples were grown on Si(100) and Si(111) substrates with a thin SiO₂ buffer layer by thermal evapora-

^{a)}Electronic mail: vsn@iph.krasn.ru.^{b)}Electronic mail: barto@unizar.es.

tion in ultrahigh vacuum (UHV) at RT using the modernized MBE “Angara” setup.¹⁸ The base pressure in the growth chamber was 2.1×10^{-7} Pa. The component materials were evaporated from refractory (boron nitride) crucibles. The evaporation process was controlled by a computer system, which includes a hardware-software complex for the operation of the UHV and of the evaporators block.¹⁸ The growth rate was monitored *in situ* by a high-speed laser ellipsometer LEF-751M, and was 0.3 nm/min for iron and 1.4 nm/min for silicon. The films investigated are Si(*hkl*)/SiO₂/Fe(*d*)/Si(1.5 nm)/Fe(*d*)/Si(1.5 nm)/Fe(*d*)/Si(10 nm) with various values of d_{Fe} (1.2, 1.6, 2.6, and 3.8 nm). Additional checks of the thickness of the Fe layers were carried out *ex situ* by x-ray fluorescence analysis. The compositions of the layers deposited were studied by Auger electron spectroscopy and electron energy loss spectroscopy.¹⁸ The small-angle x-ray scattering (SAXS) data for the multilayer (Fe/Si)_{*n*} films obtained revealed typical superlattice peaks. The composition modulation periods (from SAXS) are in good agreement with the values determined using such experimental parameters as the evaporation time and the growth rate.¹⁹

The magnetic measurements on (Fe/Si)_{*n*} were carried out using a SQUID magnetometer with applied fields up to 50 kOe. The measurements in the temperature range from 4.2 to 400 K were done with the standard plastic straw sample holder. From 300 to 800 K the oven option was used with the sample holder consisting of a twisted thin aluminum foil sheet where the sample is located in the middle of the resulting rod.²⁰ In the SQUID the sample was held in a helium atmosphere of 2 mbar pressure providing clean annealing and *in situ* measurements during the annealing.

The easy axis of magnetization is parallel to the film plane at zero field, as evidenced by the typical rectangular magnetization hysteresis loops measured with applied field *H* parallel to the film plane. The value of the coercivity for the samples ranges from 60 to 200 Oe.¹⁰ The magnetization *M* versus temperature *T* measurements for (Fe/Si)_{*n*} multilayers were carried out in the external field *H*=700 Oe sufficient to guarantee magnetic saturation.¹⁴ The diamagnetic contribution, determined in an independent measurement on a blank substrate, was subtracted from the data.

The values of the magnetization of the α -phase in the Fe–Si system are in the range of 1200 Gs (Fe₃Si) to 1700 Gs (Fe).²¹ Thus, reduction in the magnetization below these values is caused by the formation of nonmagnetic phases (silicide); therefore, the amount of nonmagnetic phases is proportional to the loss of magnetization.

III. RESULTS AND DISCUSSION

The temperature dependence of magnetization is presented in the Fig. 1. Magnetization is calculated as the ratio of the total magnetic moment of the sample to the total volume of Fe in the film. It is evident that both the absolute magnetization value and its temperature dependence are different in films with various d_{Fe} ; with decreasing d_{Fe} the value of magnetization at *T*=0, (*M*₀) decreases, and the slope of the low temperature dependence increases. The *M*(*T*) curves

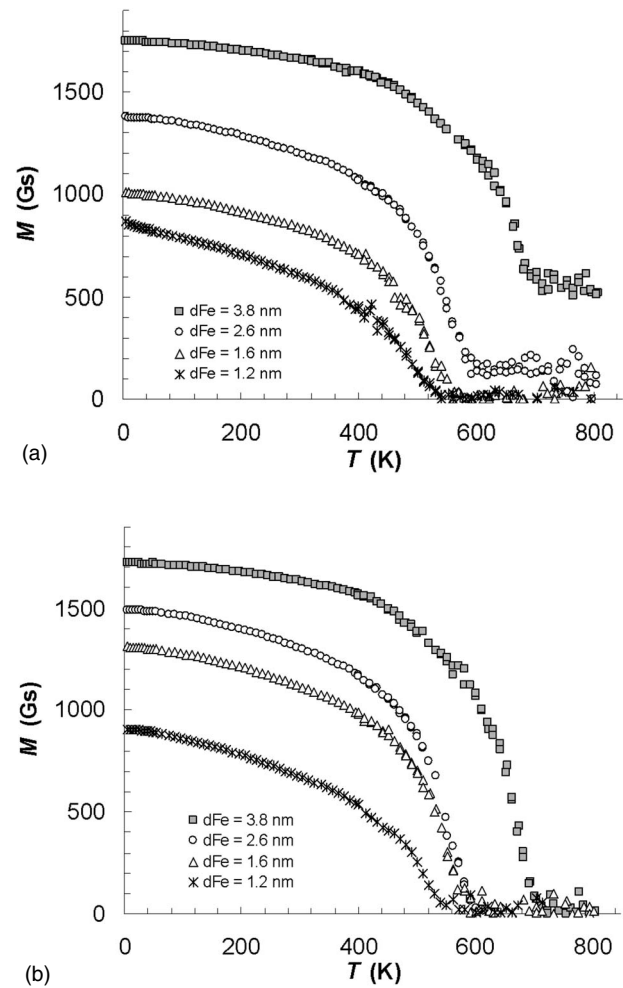


FIG. 1. The magnetization *M*(*T*) as a function of temperature (in heating process) of the Si(*hkl*)/SiO₂/Fe(*d*)/Si(1.5 nm)/Fe(*d*)/Si(1.5 nm)/Fe(*d*)/Si(10 nm) samples. (a) Si(100) substrate. (b) Si(111) substrate.

are different for films prepared on substrates of silicon cut along different crystallographic orientations, (100) and (111). The common feature of all *M*(*T*) dependence is the irreversible magnetization behavior above a temperature *T*_{*S*} in the range of 400–650 K (Fig. 2). The films deposited on Si(111) (for all films with different values of d_{Fe}) and some films on Si(100) (d_{Fe} =1.2 and 1.5 nm) become nonmagnetic after high temperature measurements above *T*_{*f*} (*T*_{*f*} is the temperature of α -Fe phase disappearance in the process of nonmagnetic silicide formation); i.e., after long annealing at these temperatures and subsequent cooling to RT the films are nonmagnetic. In contrast, for the films deposited on Si(100) with d_{Fe} =2.5 and 3.8 nm the magnetization is nonzero after cooling from high temperatures; i.e., after the irreversible transformation in these films some amount of the magnetic phase still remains. The irreversible reduction in magnetization at high temperatures (above *T*_{*S*}) is caused by the formation of nonmagnetic silicides. It should be noted that the *M*(*T*) behavior above *T*_{*S*} and *T*_{*f*} value will be affected by the rate of heating, which was 5 K/min for the curves presented in Fig. 1.

The difference between the properties found for (Fe/Si)_{*n*} deposited on Si(100) and Si(111) substrates is characteristic

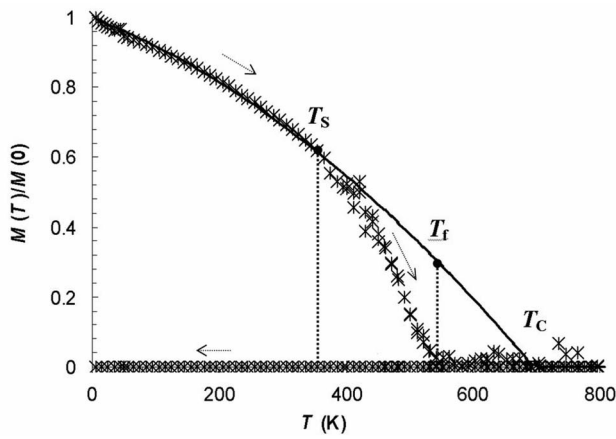


FIG. 2. The typical magnetization dependence on temperature for the sample Si(111)/SiO₂/Fe(1.2 nm)/Si(1.5 nm)/Fe(1.2 nm)/Si(1.5 nm)/Fe(1.2 nm)/Si(10 nm). Solid curve corresponds to the spin-wave theory fitted to the data below 400 K and extrapolated above. The arrows indicate the heating and cooling thermal processes. T_S is the onset temperature of the irreversible formation of silicides and T_f is the end temperature of complete transformation. T_C is the predicted Curie temperature in the absence of the transformation process.

and reproducible. It seems surprising, because usually the Si(100) and Si(111) wafers are covered with native amorphous silicon oxide, which should result in the same behavior. We can explain this behavior in the growth studies as follows. For the thick samples with $d_{\text{Fe}}=2.5$ and 3.8 nm the amount of Fe and Si atoms is such that after all chemical transformations the two phase mixture of the nonmagnetic iron silicide and the magnetic $\text{Fe}_{1-x}\text{Si}_x$ solid solution with the bcc Fe structure is formed according to the equilibrium Fe–Si phase diagram. For films with $d_{\text{Fe}}=1.6$ and 1.2 nm the composition should fall in the phase diagram region of the mixture of two nonmagnetic silicides, FeSi and FeSi₂. The data of Fig. 1(a) for Si(100) are in full agreement with these arguments. Nevertheless for the films on the Si(111) there is no magnetic phase after heating for any d_{Fe} . This suggests that in this case there is some external source of Si atoms and we think that it is the substrate itself. The lower quality of the Si(111) surface morphology, in our opinion, may result in pinholes in the silicon oxide native layer, and the extra Si atoms penetrate through these pinholes into the Fe–Si interface. The better quality of the Si(100) surface prevents this process for the Si(100) substrate.

The reversible $M(T)$ dependence in the range of temperatures from 4.2 K up to 400 K has been studied in detail in Ref. 10. The experimental curve has been fitted with the expression

$$M(T) = M_0(1 - BT^{3/2} - CT^{5/2}), \quad (1)$$

where the thermal reduction in magnetization is due to excitation of thermal magnons. It allows the determination of such parameters as the magnetization M_0 at 0 K and the value of the Fe–Fe exchange constant. In Fig. 3 the values of M_0 versus d_{Fe} are shown. The decrease in M_0 with decreasing d_{Fe} is a result of the formation of Fe silicide compounds at the Fe/Si interfaces during the synthesis. The other reason for M_0 suppression may be the antiferromagnetic interlayer exchange coupling, which is known for the Fe/Si/Fe struc-

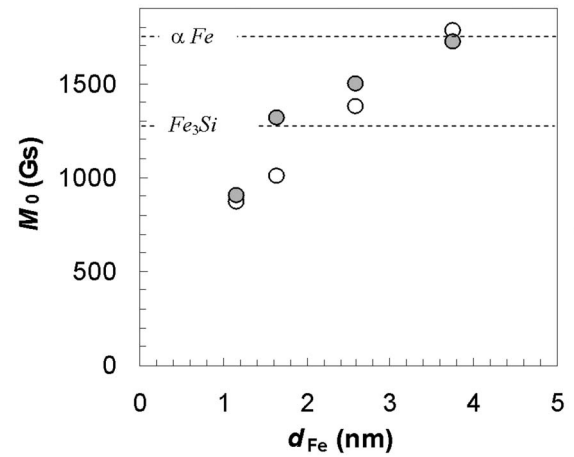


FIG. 3. The saturation magnetization at $T=0$ K, M_0 , for the different samples with varying d_{Fe} . (○) Multilayers deposited on Si(100) (●) Multilayers deposited on Si(111). (—) Saturation magnetization of bulk α -Fe and Fe₃Si.

ture and has also been detected in our samples by magnetic resonance measurements.⁶ However in this work we measure the magnetization in an external magnetic field sufficiently strong so as to overcome the antiferromagnetic coupling.

The diffusion coefficients at RT in the Fe–Si system are (in decreasing order): the diffusion of Fe in Si (Ref. 22) ($\sim 7 \times 10^{-15}$ cm²/s), the diffusion of Si in α -Fe (Ref. 11) ($\sim 8 \times 10^{-36}$ cm²/s), and the self-diffusion of Fe in α -Fe (Ref. 11) ($\sim 1 \times 10^{-47}$ cm²/s). The characteristic time of Fe diffusion in Si to a depth of ~ 1 nm is of the order of several seconds at RT. It assumes that the primary process in our samples during synthesis is Fe diffusion into Si, which results in the iron silicide formation. It is most probable that all Si atoms of the silicon spacers (1.5 nm) participate in iron silicide formation. Besides, silicide formation at high temperatures is also originated by the diffusion of Si (from the top layer of ~ 10 nm) into the reaction zone through the already formed silicide layers.²³ The enthalpies of formation for the two silicides FeSi and FeSi₂ are equal to -8.8 and -6.2 kcal/mol, respectively;¹¹ therefore the formation of FeSi is more probable.

The value of magnetization M_0 can be expressed in terms of the nonmagnetic silicides volume fraction x as follows:

$$M_0 = M_{\text{bcc}}(1 - x), \quad (2)$$

where M_{bcc} is the magnetization of α -phase of iron. Using the value $M_{\text{bcc}}=1740$ Gs and the values of M_0 in Fig. 3, we have estimated the volume fraction of nonmagnetic silicides x , which have been formed during the synthesis (Table I).

TABLE I. Volume fraction of nonmagnetic silicides x for the samples with Si substrate cut along the indicated crystallographic directions at RT.

	d_{Fe} (nm)			
	1.2	1.6	2.6	3.8
x on Si(100)	0.50	0.42	0.21	0.00
x on Si(111)	0.48	0.25	0.14	0.01

Here $x = V_{\text{silicide}}/V_{\text{film}}$ and the d_{Fe} increase at constant silicide volume results in a decrease in x . The deviation of this decrease from $1/d_{\text{Fe}}$ dependence indicates that the volume of nonmagnetic silicide itself depends on d_{Fe} . We relate the negligibly small values of x for $d_{\text{Fe}}=3.8$ nm to the better quality of the thicker layers, where the presence of fewer structural defects impedes the diffusion. Below, we discuss the activation energy versus d_{Fe} dependence that supports this argument. For $d_{\text{Fe}}=3.8$ nm the diffusion activation energy is almost twice as large as the same energy for $d_{\text{Fe}}=1.2$ nm.

Heating the sample above T_S brings on a second process involving nonmagnetic phase formation. The ensuing decrease in the average magnetization is generally caused by two mechanisms: (a) The “magnetic” one is the equilibrium reversible magnetization dependence from $T=0$ K to $T=T_C$ of any ferromagnet. Its value will not depend on the experimental measurement time (this mechanism is the unique reason for the reduction in magnetization at low temperatures). (b) The “chemical” one is the reaction producing nonmagnetic phases at the expense of the magnetic fraction, and it is irreversible. As a consequence, above T_S , the magnetization decreases with both increasing time and increasing temperature.

To separate the magnetic and chemical contributions to the experimental data, the following method was applied:

- Normalization of the value of M as $m = M/M(0)$.
- Use of a power function $m_1(T)$ (solid line in Fig. 2) satisfying the following boundary conditions: $m_1(0) = 1$, $m_1(T_C) = 0$, and $m_1(T)$, fits the reduction of magnetization in the temperature range from 0 to 300 K.
- Calculate the value $X' = (m_1(T) - m(T))/m_1(T)$, which is equal to the volume fraction of the nonmagnetic phase.

The $m_1(T)$ and X' values depend on the choice of T_C . There are different ways to estimate T_C for our films. We obtain the estimation of T_C by extrapolation of $M(T) = M_0(1 - BT^{3/2} - CT^{5/2})$ to zero magnetization (using B and C from our recent work.¹⁰) As a matter of fact the polynomial expression above should be correct at low temperatures (at high temperatures magnetization should decrease abruptly), and one can expect that the T_C values obtained will be larger than the true T_C value. So there is a range of T_C from $\max(T_C)$ (extrapolated from the low temperature reversible $M(T)$ curve) to T_f that will be less than T_C in any case. For further estimations we assume $T_C = \max(T_C)$ for all films except $d_{\text{Fe}}=3.8$ nm. For the films with $d_{\text{Fe}}=3.8$ nm the spin wave extrapolation results in $T_C=1500$ K, which is physically meaningless. We assume here that $T_C=1040$ K (the value for the α -Fe). The dependences of the resulting characteristic temperatures T_C , T_f , and T_S versus d_{Fe} are presented in Fig. 4.

The typical experimental $X'(t, T)$ dependence for the film with $d_{\text{Fe}}=1.2$ nm [on Si(100)] is shown in Fig. 5. In this experiment the temperature increase was kept at a constant rate ($T = T_0 + \alpha t$) where t is the time elapsed from the beginning of the warming process, and T_0 is the sample temperature at $t=0$. The value of t_f in Fig. 5 is the time taken for the magnetic phase to disappear. The rate of silicide synthesis is

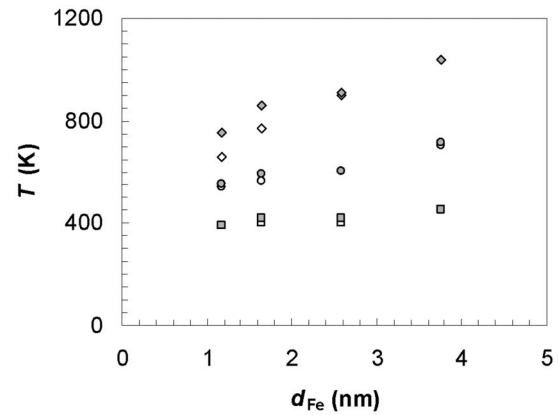


FIG. 4. The characteristic temperatures obtained from $M(T)$ curves. (\diamond) Estimation of Curie temperature T_C , (\circ) T_f , and (\square) T_S . White symbols correspond to the films on Si(100) and gray symbols correspond to the films on Si(111).

determined by the diffusion of Si atoms through the silicide layer formed.²³ It is then reasonable to consider the hypothesis that the thickness of the nonmagnetic silicide film $d(t)$ is directly related to the kinetic equation for diffusion, thus, $d(t) = [Dt]^{1/2}$, where $D = D_0/4$ is the diffusivity. The thermal activation law for the diffusivity is $D = D_0 \exp(-E_a/k_B T)$, and since in this particular experiment $T = T_0 + \alpha t$, one obtains

$$d(t) = \{D_0 \exp[-E_a/k_B(T_0 + \alpha t)]t\}^{1/2}, \quad (3)$$

with the boundary condition $d(0) = 0$ and $d(t_f) = 3\kappa d_{\text{Fe}}$ (κ is the ratio of the Fe and silicide densities). Here D_0 is the diffusion constant, E_a is the activation energy, k_B is the Boltzmann constant, $\alpha = 5$ K/min is the rate of heating, t_f is the time of full synthesis, and $d(t)$ is the thickness of the silicide layer formed.

The function $X''(t) = d(t)/d(t_f)$ is then obtained from Eq. (3) and varies from $X''(0) = 0$ and $X''(t_f) = 1$. It was fitted to the experimental data (dashed line in Fig. 5) and the values of D_0 and E_a for the films investigated with different d_{Fe} have been determined (Fig. 6).

To check the reliability of this method, direct measurements of the magnetization versus time at constant temperatures of 525, 550, and 575 K have been carried out for the

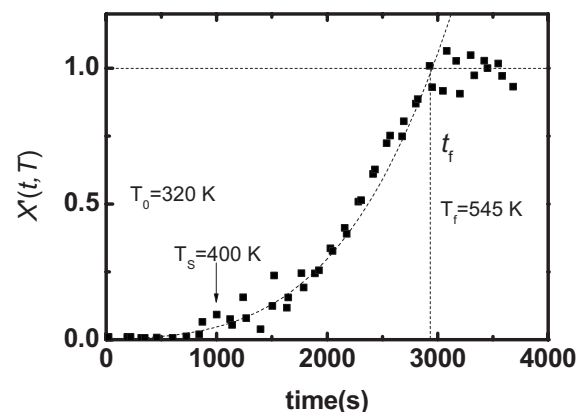


FIG. 5. The evolution of the nonmagnetic fraction with time in the sample Si(100)/SiO₂/Fe(1.2 nm)/Si(1.5 nm)/Fe(1.2 nm)/Si(1.5 nm)/Fe(1.2 nm)/Si(10 nm). t_f and T_f are the elapsed time and temperature until complete disappearance of the magnetic phases, respectively.

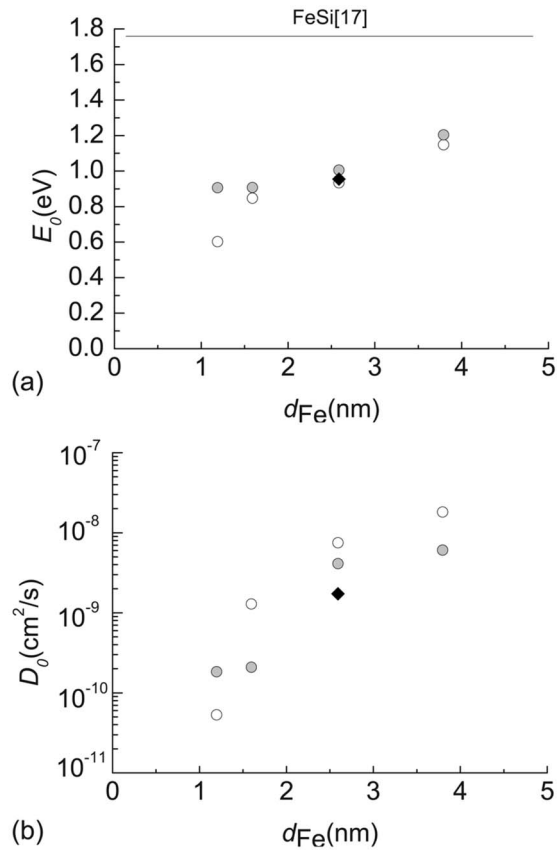


FIG. 6. (a) The activation energy and (b) the prefactor of the Si diffusion process [Eq. (3)] in the different samples. (○) Multilayers deposited on Si(100). (●) Multilayers deposited on Si(111). (◆) Values deduced from the $M(t)$ measurements at fixed temperature. (—) Activation energy of the bulk FeSi (Ref. 17).

film with $d_{Fe}=2.6$ nm. The results of these isothermal measurements are presented in Fig. 7 as M versus $t^{1/2}$. This plot indicates that the M value, whose decrease is given by $d(t)$, is proportional to $t^{1/2}$. That is, the thickness of the nonmagnetic silicide film $d(t)$ is directly related to the kinetic equa-

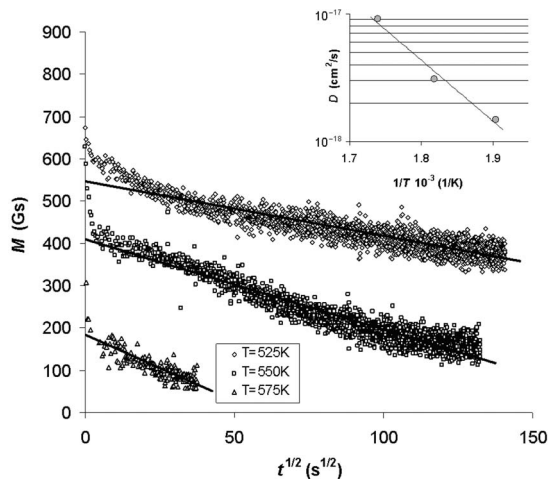


FIG. 7. Time evolution of the magnetization at fixed temperature, after an abrupt heating from the RT to the desired temperature. Note that up to 200 s there was a rapid warm up from RT to the starting temperature of the fixed reaction process. Inset: the diffusion constant, as derived from the fit of the measured curves with Eq. (5).

tion for diffusion ($d(t)=[Dt]^{1/2}$). Thus we determine the values of D ($D=d(t)^2/t$) for all temperatures and plot D versus $1/T$ (see the inset in Fig. 7). Using the expression $D=D_0 \exp(-E_a/k_B T)$ we have determined the values of D_0 and E_a directly. These values of $D_0=1.67 \times 10^{-9} \text{ cm}^2/\text{s}$ and $E_a=0.94 \text{ eV}$ are in reasonable agreement with the values obtained by fitting our experimental data to Eq. (3) (see Fig. 6).

The low activation energies in comparison with the bulk value¹⁷ (see Fig. 6) is caused by the high concentration of structural defects in the films investigated. The value of E_a increases with increasing d_{Fe} and at large d_{Fe} it seems to tend toward the value for silicide synthesis in bulk layers of iron and silicon.¹⁷ A similar conclusion is confirmed by the dependence of $M(T)$ on d_{Fe} below RT studied on the same samples,¹⁰ where it was found that the exchange constant decreases from the bulk value with decreasing d_{Fe} . The activation energy and the exchange constant are determined by the short range order. Thus, a similar thickness dependence of these parameters corroborates the point of view that the main source of structural defects in the nanolayers investigated is at the interface.

IV. CONCLUSIONS

Analysis of our *in situ* high temperature annealing measurements reveals the irreversible process that starts in the temperature range of 400–650 K due to the formation of nonmagnetic silicides, causing modification of the magnetic properties of the sample. Indeed, the magnetization at RT, after cooling from the high temperature region, is totally lost for all Fe layers on a Si(111) substrate, and for thin Fe layers below 2.5 nm on a Si(100) substrate. In contrast, for an Fe layer thickness larger than 2.5 nm on a Si(100) substrate, the RT magnetization is decreased but does not vanish.

The temperature and time dependence of the magnetization could be correlated due to the results of the *in situ* method; this correlation allows us to determine the kinetic parameters for the solid phase reaction producing iron silicide formation at the interface. The lower activation energies found in the films in comparison with the bulk are related to the higher defect concentration at the interface. With increasing Fe layer thickness we observe that the value of the activation energy seems to tend toward the value found for silicide synthesis in bulk layers of iron and silicon. The degree of silicide formation is strongly dependent on the crystalline quality of the multilayers and in particular on the interface roughness and structure. Therefore, the tendency for silicide formation is quite different for samples of different structural quality. The kinetic parameters for the silicide formation found here are related to our polycrystalline samples and are not universal for all types of Fe/Si multilayers. Nevertheless, the *in situ* method to study the magnetic properties by measurement of the high temperature SQUID measurements as Fe silicides form is universal.

Usually, in the course of device fabrication additional heating is often unavoidable, and a correct knowledge of the limiting temperature before an irreversible modification of the magnetic properties sets in is of paramount importance.

Therefore, we expect that the applied physics community will gain from the knowledge of the silicide formation kinetics in Fe/Si thin interface.

ACKNOWLEDGMENTS

This work was supported by the Russian Academy of Science program “Spintronics,” the complex integration project of the Siberian Branch of the Russian Academy of Science №3.5, the Russian Foundation for Basic Research (Grant No. 07-03-00320), the “Ramon y Cajal” program, and Project No. MAT 2005/01272 of the Spanish Ministry of Education and Science.

- ¹M. N. Baibich, J. M. Broto, A. Fert, F. Nguyen Van Dau, F. Petroff, P. Eitenne, G. Creuzet, A. Friederich, and J. Chazelas, *Phys. Rev. Lett.* **61**, 2472 (1988).
- ²R. E. Camley and R. L. Stamps, *J. Phys.: Condens. Matter* **5**, 3727 (1993).
- ³I. K. Schuller, S. Kim, and C. Leighton, *J. Magn. Magn. Mater.* **200**, 571 (1999).
- ⁴G. S. Patrin, N. V. Volkov, and V. P. Kononov, *Pis'ma Zh. Eksp. Teor. Fiz.* **68**, 287 (1998) [*JETP Lett.* **68**, 307 (1998)].
- ⁵G. S. Patrin, S. G. Ovchinnikov, D. A. Velikanov, and V. P. Kononov, *Fiz. Tverd. Tela (S.-Peterburg)* **43**, 1643 (2001) [*Phys. Solid State* **43**, 1712 (2001)].
- ⁶G. S. Patrin, N. V. Volkov, S. G. Ovchinnikov, E. V. Eremin, M. A. Panova, and S. N. Varnakov, *Pis'ma Zh. Eksp. Teor. Fiz.* **80**, 560 (2004); [*JETP Lett.* **80**, 491 (2004)].
- ⁷G. J. Strijkers, J. T. Kohlhepp, H. J. M. Swagten, and W. J. M. de Jonge, *Phys. Rev. Lett.* **84**, 1812 (2000).
- ⁸R. R. Gareev, D. E. Bürgler, M. Buchmeier, D. Olligs, R. Schreiber, and P.

- Grünberg, *Phys. Rev. Lett.* **87**, 157202 (2001).
- ⁹D. E. Bürgler, M. Buchmeier, S. Cramm, S. Eisebitt, R. R. Gareev, P. Grünberg, C. L. Jia, L. L. Pohlmann, R. Schreiber, M. Siegel, Y. L. Qin, and A. Zimina, *J. Phys.: Condens. Matter* **15**, S443 (2003).
- ¹⁰S. N. Varnakov, J. Bartolomé, J. Sesé, S. G. Ovchinnikov, S. V. Komogortsev, A. S. Parshinn, and G. V. Bondarenko, *Fiz. Tverd. Tela (S.-Peterburg)* **49**, 1401 (2007) [*Phys. Solid State* **49**, 1470 (2007)].
- ¹¹C. J. Smithells, *Metals Reference Book* (Butterworths, London, 1967), Vols. 1–3.
- ¹²J. E. Mattson, S. Kumar, E. E. Fullerton, S. R. Lee, C. H. Sowers, M. Grimsditch, S. D. Bader, and F. T. Parker, *J. Appl. Phys.* **75**, 6169 (1994).
- ¹³M. Yu. Gomoyunova, I. I. Pronin, D. E. Malygin, S. M. Solov'ev, D. V. Vyalykh, and S. L. Molodtsov, *Zh. Tekh. Fiz.* **75**, 106 (2005) [*Tech. Phys.* **50**, 1212 (2005)].
- ¹⁴G. J. Strijkers, J. T. Kohlhepp, H. J. M. Swagten, and W. J. M. de Jonge, *Phys. Rev. B* **60**, 9583 (1999).
- ¹⁵T. Lucinski, M. Kopcewicz, A. Hütten, H. Brückl, S. Heitmann, T. Hempel, and G. Reiss, *J. Appl. Phys.* **93**, 6501 (2003).
- ¹⁶J. M. Gallego and R. Miranda, *J. Appl. Phys.* **69**, 1377 (1991).
- ¹⁷S. S. Lau, J. S.-Y. Feng, J. O. Olowolafe, and M.-A. Nicolet, *Thin Solid Films* **25**, 415 (1975).
- ¹⁸S. N. Varnakov, A. A. Lepeshev, S. G. Ovchinnikov, A. S. Parshin, M. M. Korshunov, and P. Nevoral, *Prib. Tekh. Eksp.* **6**, 252 (2004) [*Instrum. Exp. Tech.* **47**, 839 (2004)].
- ¹⁹S. N. Varnakov, A. S. Parshin, S. G. Ovchinnikov, D. Rafaja, L. Kalvoda, A. D. Balaev, and S. V. Komogortsev, *Pis'ma Zh. Tekh. Fiz.* **31**, 1 (2005) [*Tech. Phys. Lett.* **31**, 947 (2005)].
- ²⁰J. Sesé, J. Bartolomé, and C. Rillo, *Rev. Sci. Instrum.* **78**, 046101 (2007).
- ²¹*Magnetic Properties of Metals: D-Elements, Alloys and Compounds*, edited by H. P. J. Wijn (Springer, Berlin, 1991), p. 190.
- ²²D. Gilles, W. Schröter, and W. Bergholz, *Phys. Rev. B* **41**, 5770 (1990).
- ²³M. Ohring, *The Materials Science of Thin Films* (Academic, New York, 1992), p. 704.